Ultra-relativistic heavy-ion collisions: Lecture II

Wojciech Florkowski[1,2]

[1] Jan Kochanowski University, Kielce, Poland
[2] Institute of Nuclear Physics, Polish Academy of Sciences, Kraków, Poland

48th Karpacz Winter School of Theoretical Physics
Lądek–Zdrój, February 4–11, 2012

Outline

LECTURE I

1. Introduction

   1.1 High-energy nuclear collisions
   1.2 Theoretical methods
   1.3 Quantum chromodynamics
   1.4 Quark-gluon plasma
   1.5 Chiral symmetry
   1.6 Hot and dense nuclear matter

2. Basic Dictionary

   2.1 Participants, spectators, and impact parameter
   2.2 Kinematical variables
   2.3 Centrality
   2.4 Reaction plane
   2.5 Collective flows
   2.6 Stopping and transparency
   2.7 Boost invariance

Outline

LECTURE II

Outline

STANDARD MODEL (MODULES) of HEAVY−ION COLLISIONS

initial conditions → **hydro expansion** → **hadronic freeze−out**

thermalization

Glauber or CGC   perfect or viscous   free−streaming or hadronic cascade
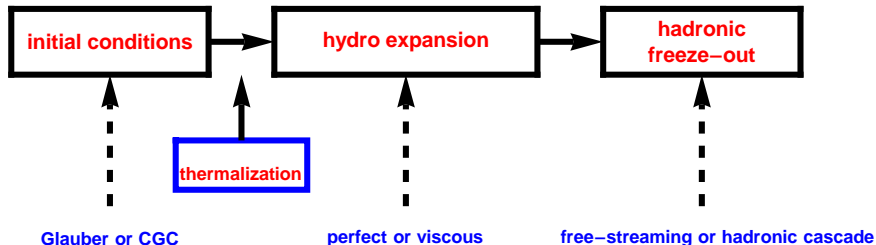
NEW: FLUCTUATIONS IN THE INITIAL STATE / EVENT−BY−EVENT HYDRO / FINAL−STATE FLUCTUATIONS

EQUATION OF STATE?

VISCOSITY?

3. GLAUBER MODEL

Roy Glauber
receiving Nobel Prize
Stockholm, Dec. 2005.

In realistic situations the separation between spectators and participants is not so sharp as in the simple geometric picture introduced earlier.

A more elaborate estimate of the number of participating nucleons can be done within the **Glauber model** which **treats a nucleus-nucleus collision as a multiple nucleon-nucleon collision process**.

In the Glauber model, **the nucleon distributions in nuclei are random and given by the nuclear density profiles**

whereas the **elementary nucleon-nucleon collision is characterized by the total inelastic cross section** σ_{in}.
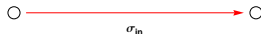
Initially, the Glauber model was applied only to elastic collisions. In this case a nucleon does not change its properties in the individual collisions, so all nucleon interactions can be well described by the same cross section.
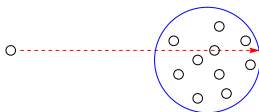
Applying the Glauber model to inelastic collisions, we assume that after a single inelastic collision an excited nucleon-like object is created that interacts basically with the same inelastic cross section with other nucleons.
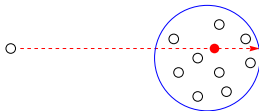
3.1 Eikonal approximation

The **eikonal approximation is the classical approximation to the angular momentum**. It may be applied to the standard expansion of the elastic scattering amplitude into the angular-momentum eigenstates defined by the orbital number l,

$$f(s, t) = \frac{1}{2ip} \sum_l (2l + 1) \left[e^{2i\delta_l} - 1 \right] P_l(\cos \theta). \tag{1}$$

Here s and t are the Mandelstam variables, i.e., the center-of-mass energy squared and the invariant momentum transfer squared,

$$s = (p_1 + p_2)^2 = 4(m^2 + p^2), \qquad t = (p_1 - p_1')^2 = \frac{1}{2}(\cos \theta - 1)(s - 4m^2). \tag{2}$$

High-energy elastic scattering processes are far from being spherically symmetric, hence the **large values of l dominate in (1)** and we may write

$$p\,b = l + \frac{1}{2}, \tag{3}$$

where b is the impact parameter. For large l and small scattering angles θ the **Legendre polynomial $P_l(\cos \theta)$ may be approximated by the formula**

$$P_l(\cos \theta) = \int\limits_0^{2\pi} \frac{d\phi}{2\pi} e^{i(2l+1)\sin(\theta/2)\cos(\phi)}. \tag{4}$$

3.1 Eikonal approximation
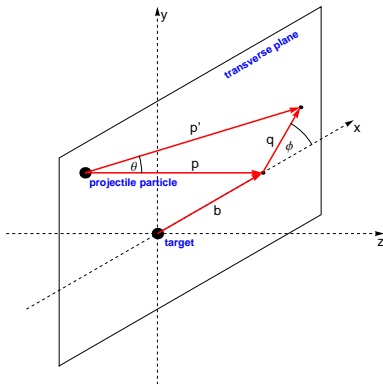
At high energy, the momentum transfer vector $\mathbf{q} = \mathbf{p}' - \mathbf{p}$ lies in the transverse plane, and we may rewrite the argument of the exponential function in (4) as a scalar product of $\mathbf{q}$ and $\mathbf{b}$,

$$(2l + 1) \sin\left(\frac{\theta}{2}\right) \cos(\phi) \tag{5}$$
$$= 2p \sin\left(\frac{\theta}{2}\right) \frac{l + 1/2}{p} \cos(\phi) = \mathbf{q} \cdot \mathbf{b}.$$

In this way we find the simple representation

$$P_l(\cos\theta) = \int_0^{2\pi} \frac{d\phi}{2\pi} e^{i\mathbf{q} \cdot \mathbf{b}}. \tag{6}$$

3.1 Eikonal approximation

After replacing l by b we may treat b as the continuous variable (with $db = dl/p$ and $d^2b = b \, db \, d\phi$). In this approximation, the scattering amplitude has the form

$$f(s, \mathbf{b}) = \frac{ip}{2\pi} \int d^2b \, e^{i\mathbf{q}\cdot\mathbf{b}} \left[1 - e^{i\chi(s,\mathbf{b})} \right], \quad \chi(s, \mathbf{b}) = 2\,\delta(s, \mathbf{b}). \tag{7}$$

The **total cross section** may be obtained from the **forward scattering amplitude** with the help of the **optical theorem**

$$\sigma_{\text{tot}} = \frac{4\pi}{p} \text{Im} \, f(s, t = 0) = 2 \int d^2b \left[1 - \text{Re} \, e^{i\chi(s,\mathbf{b})} \right]. \tag{8}$$

3.1 Eikonal approximation

The **elastic cross section** is obtained by squaring the amplitude and integrating over the solid angle. Since the scattering is concentrated in the forward direction, the integration over the solid angle may be replaced by the integral over the space orthogonal to the momentum vector **p**,

$$d\Omega = \frac{d^2q}{p^2}. \tag{9}$$

Using this property we obtain

$$
\begin{aligned}
\sigma_{\mathrm{el}} &= \int \frac{d^2q}{4\pi^2} \int d^2b \int d^2b' \, e^{i\mathbf{q}\cdot\mathbf{b}} \left[1 - e^{i\chi(s,\mathbf{b})}\right] e^{-i\mathbf{q}\cdot\mathbf{b}'} \left[1 - e^{i\chi(s,\mathbf{b}')}\right]^* \\
&= \int d^2b \left|1 - e^{i\chi(s,\mathbf{b})}\right|^2.
\end{aligned}
\tag{10}
$$

Finally, the **inelastic cross section** is

$$\sigma_{\mathrm{in}} = \sigma_{\mathrm{tot}} - \sigma_{\mathrm{el}} = \int d^2b \left(1 - \left|e^{i\chi(s,\mathbf{b})}\right|^2\right) \equiv \int d^2b \, p(\mathbf{b}). \tag{11}$$

3.2 Nucleon-nucleon collisions

At high energies, the inelastic cross section gives the main contribution to the total cross section.

A certain subclass of the inelastic processes is the **diffractive dissociation** process. In this process a nucleon is only slightly excited and a small number of particles is produced, which is in contrast to the typical **non-diffractive inelastic** events. The diffractive processes represent about 10% of all inelastic collisions.
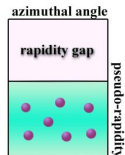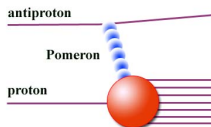
Schematic diagrams of proton-antiproton single diffraction and double pomeron exchange.

3.2.1 Nucleon-nucleon collisions: energy dependence

In non-diffractive inelastic nucleon-nucleon collisions a certain number of charged particles is produced. The **average charged particle multiplicity** may be described by the phenomenological formula

$$\overline{N}_{\mathrm{NN}} = 0.88 + 0.44 \ln \frac{s}{s_0} + 0.118 \left(\ln \frac{s}{s_0} \right)^2, \tag{12}$$

where s_0 = 1 GeV. Another phenomenological formula may be used to describe the average charged particle multiplicity at midrapidity

$$\left. \frac{d\overline{N}_{\mathrm{NN}}}{d\eta} \right|_{\eta=0} = 2.5 - 0.25 \ln \frac{s}{s_0} + 0.023 \left(\ln \frac{s}{s_0} \right)^2. \tag{13}$$

Equation (13) is a parametrization of the $p\overline{p}$ data obtained by the UA5 and the CDF group in the range 50 GeV $< \sqrt{s} <$ 2000 GeV.

3.2.1 Nucleon-nucleon collisions: energy dependence

NEWS from the LHC: power-law behavior!
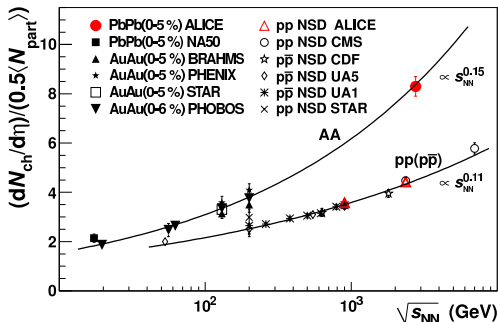
3.2.2 Nucleon-nucleon collisions: thickness function

Let us consider a nucleon-nucleon collision at a given energy $\sqrt{s}$ and at an impact parameter b. According to our discussion presented before, we may introduce the **probability of having a nucleon-nucleon inelastic collision**

$$p\left(\mathbf{b}\right) = \left(1 - \left|e^{i\chi(\mathbf{b})}\right|^2\right) \equiv t\left(\mathbf{b}\right)\sigma_{\mathrm{in}}. \tag{14}$$

The function $t\left(\mathbf{b}\right)$, defined by (14), is called the nucleon-nucleon **thickness function**. The integral of $p\left(\mathbf{b}\right)$ over the whole range of the impact parameter should be normalized to σ_{in}. Thus, the thickness function is normalized to unity

$$\int d^2b\, t\left(\mathbf{b}\right) = 1. \tag{15}$$

For collisions with unpolarized beams $t\left(\mathbf{b}\right)$ depends only on the magnitude of $\mathbf{b}$.

3.3.1 Nucleon-nucleus collisions: density profiles

The probability of finding a nucleon in the nucleus with the atomic mass number *A* is the usual baryon density divided by the number of baryons in the nucleus (our definition of $\rho_A(r)$ includes *A* in the denominator, because we want to interpret $\rho_A(r)$ as the probability distribution.). For large nuclei, one commonly uses the **Woods-Saxon function**

$$\rho_A(r) = \frac{\rho_0}{A\left(1 + \exp\left[\frac{r-r_0}{a}\right]\right)}, \tag{16}$$

with the parameters:

$$r_0 = (1.12A^{1/3} - 0.86A^{-1/3})\,\text{fm}, \tag{17}$$

$$a = 0.54\,\text{fm}, \tag{18}$$

and

$$\rho_0 = 0.17\,\text{fm}^{-3}. \tag{19}$$

The parameter ρ_0 is the **nuclear saturation density**.

3.3.1 Nucleon-nucleus collisions: density profiles

The **nucleon-nucleus thickness function** for the nucleus A is obtained from a simple geometric consideration (see right) and the assumption that the nucleon positions in the nucleus A are not changed during the collision process,

$$T_A(\mathbf{b}) = \int dz_A \int d^2 s_A \, \rho_A(\mathbf{s}_A, z_A) \, t(\mathbf{s}_A - \mathbf{b}). \tag{20}$$
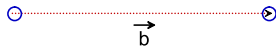
Here the transverse coordinates are denoted by the vector $\mathbf{s}_A$, and we use notation

$$\rho_A(\mathbf{s}_A, z_A) = \rho_A\left(\sqrt{\mathbf{s}_A^2 + z_A^2}\right). \tag{21}$$

Equation (15) implies the normalization condition

$$\int d^2 b \, T_A(\mathbf{b}) = 1. \tag{22}$$

a)

b)
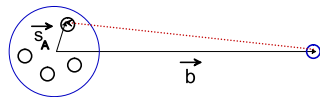
c)
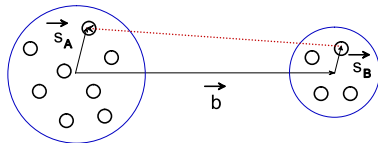
3.3.2 Nucleon-nucleus collisions: independent collisions

The quantity $T_A(\mathbf{b})\,\sigma_{\rm in}$ is the probability that a single nucleon-nucleon collision takes place in a nucleon-nucleus collision at the impact parameter $\mathbf{b}$. Treating all possible nucleon-nucleon collisions in the nucleon-nucleus collision as completely independent and characterized by the same cross section, we easily find the probability of having n such collisions. The latter is expressed by the binomial distribution

$$P(n; A; \mathbf{b}) = \left(\begin{array}{c} A \\ n \end{array} \right) [1 - T_A(\mathbf{b})\,\sigma_{\rm in}]^{A-n} [T_A(\mathbf{b})\,\sigma_{\rm in}]^n . \tag{23}$$

The **average number of binary nucleon-nucleon collisions** may be calculated from (23) which gives

$$\overline{n}(A; \mathbf{b}) = \sum_{n=1}^{A} nP(n; A; \mathbf{b}) = A\,T_A(\mathbf{b})\,\sigma_{\rm in}. \tag{24}$$

3.3.2 Nucleon-nucleus collisions: independent collisions

Since the scale at which the nucleon-nucleon thickness function varies is typically smaller than the scale at which the nuclear density changes, we may often replace $t(\mathbf{s}_A - \mathbf{b})$ in (20) by the delta function $\delta^{(2)}(\mathbf{s}_A - \mathbf{b})$. In this approximation $T_A(\mathbf{b})$ is the nuclear density projected onto the transverse plane

$$T_A(\mathbf{b}) = \int dz_A \, \rho_A(\mathbf{b}, z_A), \tag{25}$$

and the average number of the collisions is

$$\overline{n}(A; \mathbf{b}) = A \, \sigma_{\text{in}} \int dz_A \, \rho_A(\mathbf{b}, z_A). \tag{26}$$

3.4 Nucleus-nucleus collisions

Finally, we define the thickness function for the nucleus-nucleus collision. A geometric consideration leads to the formula

$$T_{AB}(\mathbf{b}) = \int dz_A \int d^2 s_A \, \rho_A(\mathbf{s}_A, z_A) \int dz_B \int d^2 s_B \, \rho_B(\mathbf{s}_B, z_B) \, t(\mathbf{b} + \mathbf{s}_B - \mathbf{s}_A), \quad (27)$$

with the corresponding normalization condition

$$\int d^2 b \, T_{AB}(\mathbf{b}) = 1. \quad (28)$$

The quantity $T_{AB}(\mathbf{b}) \, \sigma_{\rm in}$ is the **averaged** probability that a nucleon-nucleon collision takes place in a nucleus-nucleus collision characterized by the impact parameter **b**. In the limit $t(\mathbf{b}) \to \delta^{(2)}(\mathbf{b})$ we may write

$$T_{AB}(\mathbf{b}) = \int d^2 s_A \, T_A(\mathbf{s}_A) \, T_B(\mathbf{s}_A - \mathbf{b}). \quad (29)$$
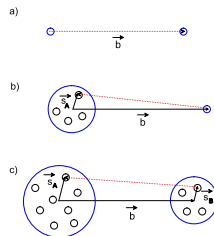
3.4 Nucleus-nucleus collisions

In a more symmetric form we have

$$T_{AB}\left(\mathbf{b}\right) = \int d^2s\, T_A\left(\mathbf{s} + \frac{1}{2}\mathbf{b}\right)\, T_B\left(\mathbf{s} - \frac{1}{2}\mathbf{b}\right). \tag{30}$$

The nucleus-nucleus thickness function $T_{AB}\left(\mathbf{b}\right)$ can be used to calculate the probability of having n inelastic binary nucleon-nucleon collisions in a nucleus-nucleus collision at the impact parameter $\mathbf{b}$.

$$P\left(n; AB; \mathbf{b}\right) = \left(\begin{array}{c} AB \\ n \end{array}\right) \left[1 - T_{AB}\left(\mathbf{b}\right)\sigma_{\mathrm{in}}\right]^{AB-n} \left[T_{AB}\left(\mathbf{b}\right)\sigma_{\mathrm{in}}\right]^n. \tag{31}$$

The result for the average number of the collisions is

$$\overline{n}\left(AB; \mathbf{b}\right) = AB\, T_{AB}\left(\mathbf{b}\right)\sigma_{\mathrm{in}}. \tag{32}$$

3.4.1 ... total inelastic cross section

The total probability of an inelastic nuclear collision is the sum over n from $n = 1$ to $n = AB$

$$P_{\text{in}}\left(AB; \mathbf{b}\right) = \sum_{n=1}^{AB} P\left(n; AB; \mathbf{b}\right) = 1 - \left[1 - T_{AB}\left(\mathbf{b}\right)\sigma_{\text{in}}\right]^{AB}. \tag{33}$$

From (33), by integrating over the impact parameter space, one may obtain the **total inelastic cross section for the collision of the two nuclei** A **and** B

$$\sigma_{\text{in}}^{AB} = \int d^2 b \left(1 - \left[1 - T_{AB}\left(\mathbf{b}\right)\sigma_{\text{in}}\right]^{AB}\right). \tag{34}$$

Using the thickness function for the Au+Au collisions we find $\sigma_{\text{in}}^{\text{AuAu}}$ = 6.8 b for σ_{in} = 30 mb and $\sigma_{\text{in}}^{\text{AuAu}}$ = 7.0 b for σ_{in} = 40 mb. We note that those cross sections are larger than the geometric cross section $\sigma_{\text{geo}}^{\text{AuAu}} = 4\pi R^2 \approx 5\pi A^{2/3}$ = 5.3 b. This is due to the tails of the Woods-Saxon distribution (16), which make possible that a nucleon-nucleon collision occurs in the nuclear collision at the impact parameter b larger than $2R$.

3.4.1 ... total inelastic cross section

We did something wrong! We used the averaged probability for nucleon-nucleon collisions! In more realistic calculations, the positions of nucleons in the target and projectile nucleus are fixed, and the averaging is done later. The probability of an inelastic collision for a fixed nucleon configuration equals

$$1 - \prod_{j=1}^{A}\prod_{i=1}^{B}\left[1 - t\left(\mathbf{b} + \mathbf{s}_i^B - \mathbf{s}_j^A\right)\sigma_{\mathrm{in}}\right]. \tag{35}$$

The probability of an inelastic **nuclear collision** at the impact parameter **b** is then

$$
\begin{aligned}
P_{\mathrm{in}}\left(AB;\mathbf{b}\right) &= \int d^2s_1^A T_A(\mathbf{s}_1^A)\cdots d^2s_A^A T_A(\mathbf{s}_A^A)\int d^2s_1^B T_B(\mathbf{s}_1^B)\cdots d^2s_B^B T_B(\mathbf{s}_B^B)\\
&\times \left\{1 - \prod_{j=1}^{A}\prod_{i=1}^{B}\left[1 - t\left(\mathbf{b} + \mathbf{s}_i^B - \mathbf{s}_j^A\right)\sigma_{\mathrm{in}}\right]\right\}.
\end{aligned}\tag{36}
$$

The integration of (36) over b gives $\sigma_{\mathrm{in}}^{AB}$. Equations (33) and (36) differ from each other! The more accurate formula (36) is much more complicated to handle and cannot be simply reduced to (33). Only for nucleon-nucleus collisions the two methods are equivalent. Since there is no good analytic method to evaluate (36) for large values of A and B, one is most often satisfied with Eqs. (33) and (34) only. These equations are called the **optical limit of the Glauber model**.

3.5 Wounded nucleons

The Glauber model can be used also to calculate the number of the participants. To be more precise we distinguish between the **participants which may interact elastically** and the **participants which interact only inelastically**. The latter are called the **wounded nucleons**.

The number of nucleons in the nucleus A

$$A \int d^2 s \, T_A(\mathbf{s}). \tag{37}$$

Probability, that the nucleus from A at the position $\mathbf{s}$ collides one or more times with the nucleons in B (in an AB collision at the impact parameter $\mathbf{b}$)

$$\sum_{n=1}^{B} P(n; B; \mathbf{b} - \mathbf{s}) = 1 - [1 - \sigma_{\mathrm{in}} T_B(\mathbf{b} - \mathbf{s})]^B.$$

$$\tag{38}$$

The number of wounded nucleons in A is

$$\overline{w}_A(A; B; \mathbf{b}) = A \int d^2 s \, T_A(\mathbf{s}) \left(1 - [1 - \sigma_{\mathrm{in}} T_B(\mathbf{b} - \mathbf{s})]^B\right). \tag{39}$$

3.5 Wounded nucleons

Similarly, the number of wounded nucleons in *B* is

$$\overline{w}_B\left(A;B;\mathbf{b}\right) \;=\; B \int d^2 s\, T_B\left(\mathbf{s}\right)\left(1-\left[1-\sigma_{\mathrm{in}}\, T_A\left(\mathbf{b}+\mathbf{s}\right)\right]^A\right). \tag{40}$$

Since the number of wounded nucleons in the collision of *A* and *B* is the sum of the wounded nucleons in the nucleus *A* and *B*, we obtain (after making the appropriate shifts in the integration over positions **s**)

$$\begin{aligned}
\overline{w}\left(A;B;\mathbf{b}\right) \;=\;& A \int d^2 s\, T_A\left(\mathbf{b}-\mathbf{s}\right)\left(1-\left[1-\sigma_{\mathrm{in}}\, T_B\left(\mathbf{s}\right)\right]^B\right) \\
&+ B \int d^2 s\, T_B\left(\mathbf{b}-\mathbf{s}\right)\left(1-\left[1-\sigma_{\mathrm{in}}\, T_A\left(\mathbf{s}\right)\right]^A\right).
\end{aligned} \tag{41}$$

3.5.1 Wounded nucleons vs. binary collisions

The numbers of binary collisions, $\overline{n}(b)$, and the numbers of wounded nucleons, $\overline{w}(b)$, for Au+Au collisions ($A = 197$) at different values of the impact parameter b. The results are presented for two different values of the nucleon-nucleon inelastic cross section: $\sigma_{\mathrm{in}} = 30$ mb (the second and the third column), and $\sigma_{\mathrm{in}} = 40$ mb (the fifth and the sixth column). The fourth and seventh columns give geometric estimates of the centrality class of the collisions with the impact parameters **smaller** than b (the fourth column is for $\sigma_{\mathrm{in}}^{\mathrm{AuAu}} = 6.8$ b, whereas the sixth column is for $\sigma_{\mathrm{in}}^{\mathrm{AuAu}} = 7.0$ b).

b [fm]	$\overline{n}(b)$	$\overline{w}(b)$	c	$\overline{n}(b)$	$\overline{w}(b)$	c
0	881	370	0.00	1174	378	0.00
1	859	363	0.00	1146	371	0.00
2	801	344	0.02	1068	354	0.02
3	717	315	0.04	957	326	0.04
4	617	280	0.07	823	291	0.07
5	587	241	0.12	783	251	0.11
6	397	200	0.17	530	211	0.16
7	298	160	0.23	397	170	0.22
8	209	122	0.29	279	131	0.29
9	136	88	0.37	182	95	0.36
10	82	58	0.46	109	64	0.45

3.6 Soft and hard processes

It is an experimental fact that pions (the most abundant particles produced in a nucleon-nucleon as well as in a nucleus-nucleus collision) have on average small transverse momenta, $p_\perp \sim 400$ MeV. The processes leading to the production of such low-energetic pions are called **soft processes**. On the other hand, the pions with large transverse momenta, $p_\perp > 1$–2 GeV, are produced by **hard processes**.

The soft processes cannot be described directly by perturbative QCD. In this case the strong coupling constant is large and the nonperturbative effects, which very difficult to deal with, are important. Contrary, the hard processes involve large momentum transfers connected with a small value of the strong coupling constant. Hence, they can be described successfully by the methods of perturbative QCD.

3.6 Soft and hard processes

Can we use the knowledge of $\overline{w}_{AB}$ and $\overline{n}_{AB}$ to make an estimate of the multiplicity of the particles produced in a nuclear collision, provided the information about the multiplicity of the particles produced in a more elementary nucleon-nucleon collision (at the same energy) is available?

SEARCH FOR SIMPLE SCALINGS (SUPERPOSITION RULES)

For hard processes it is natural to assume that the number of the produced particles scales with the number of binary collisions. In this case the scattering processes are well localized and the interference effects between different collisions may be neglected. For soft processes the appropriate scaling is more difficult to find. In fact, it is a postulate of the wounded-nucleon model that the multiplicity of soft particles scales with the number of the wounded nucleons.

3.7 Wounded-nucleon model

Białas, Bleszyński and Czyż argued (in 1976) that the average multiplicity in a collision of two nuclei with the mass numbers A and B is

$$\overline{N}_{AB} = \tfrac{1}{2}\, \overline{w}_{AB}\, \overline{N}_{\mathrm{NN}}, \tag{42}$$

where $\overline{N}_{\mathrm{NN}}$ is the average multiplicity in proton-proton (nucleon-nucleon) collisions, and $\overline{w}_{AB}$ is the average number of the wounded nucleons (calculated in the Glauber framework). The energy dependence of $\overline{N}_{\mathrm{NN}}$ is described by (12). The motivation for the use of (42) came from the interpretation of the nucleon-nucleus interactions. The formula (42) with an additional expression for the dispersion of multiplicity distributions form the main ingredients of the **wounded-nucleon model** of the nucleus-nucleus collisions.

3.7 Wounded-nucleon model

Estimates of the charged particle multiplicities obtained from the wounded nucleon model, $\frac{1}{2} \overline{w}_{AA} \overline{N}_{\mathrm{NN}}$, compared with the measured multiplicities, $\overline{N}_{AA}$, for different reactions studied by the NA49 and PHOBOS Collaborations. The last column shows the ratio of the measured multiplicity and the model prediction.

Expt.	E_{lab}/A [GeV]	$\sqrt{s_{\mathrm{NN}}}$ [GeV]	$\overline{N}_{AA}$	$\overline{w}_{AA}$	$\frac{1}{2} \overline{w}_{AA} \overline{N}_{\mathrm{NN}}$	r
NA49	40	8.8	693	349	875	0.79
NA49	80	12.3	1029	349	1059	0.97
NA49	158	17.3	1413	362	1307	1.08
PHOBOS	(9000)	130.0	4200	355	2902	1.45

3.7 Wounded-nucleon model

The charged particle pseudorapidity density as a function of the number of the participants. The measurement of the PHENIX group at RHIC, $\sqrt{s_{NN}}$ = 130 GeV, is compared to the measurement done by the WA98 group at the SPS, $\sqrt{s_{NN}}$ = 17.3 GeV.
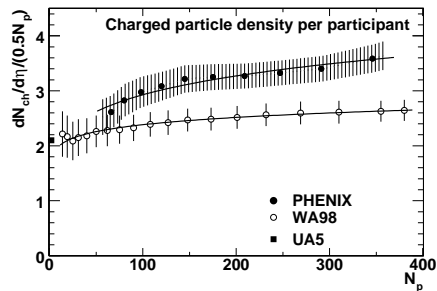
3.8 Nuclear modification factor

A simple way to quantify the differences between the nucleus-nucleus collisions and the nucleon-nucleon collisions is to calculate the **nuclear modification factor**,

$$R_{AB}(p_\perp) = \frac{1}{\overline{n}_{AB}} \frac{d^2\overline{N}_{AB}}{dp_\perp d\eta} \Big/ \frac{1}{\sigma_{\text{tot}}^{pp}} \frac{d\sigma_{\text{incl}}^{pp}}{dp_\perp d\eta}. \tag{43}$$

$\overline{N}_{AB}$ – average number of particles produced in the collisions of the nuclei A and B, $\overline{n}_{AB}$ – number of the binary nucleon-nucleon collisions obtained in the framework of the Glauber model.

The denominator of (43) is the inclusive cross section for pp collisions divided by the total cross section. This quantity is equal to the average number of particles produced in pp collisions in the appropriate phase-space interval,

$$\frac{dN_{pp}}{dp_\perp d\eta} = \frac{1}{\sigma_{\text{tot}}^{pp}} \frac{d\sigma_{\text{incl}}^{pp}}{dp_\perp d\eta}. \tag{44}$$

If the collisions of the nuclei A and B are simple superpositions of the elementary pp collisions, the scaling with the number of binary collisions should hold, and the nuclear modification factor is expected to be equal to 1.
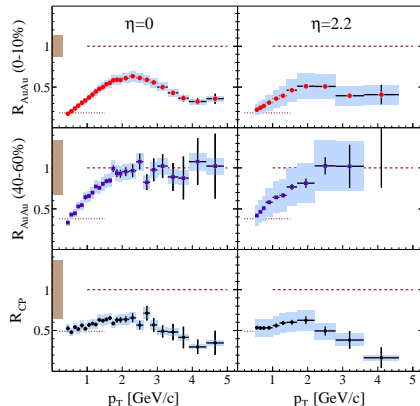
3.8 Nuclear modification factor

The nuclear modification factor R_{dAu} as measured by the PHOBOS Collaboration at BNL.
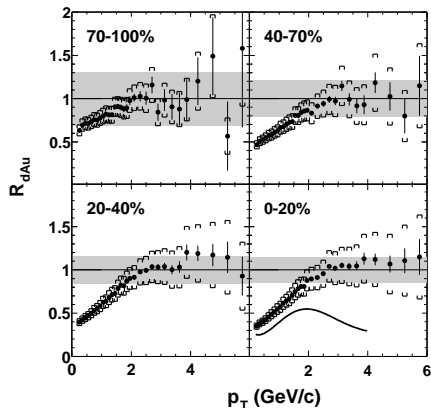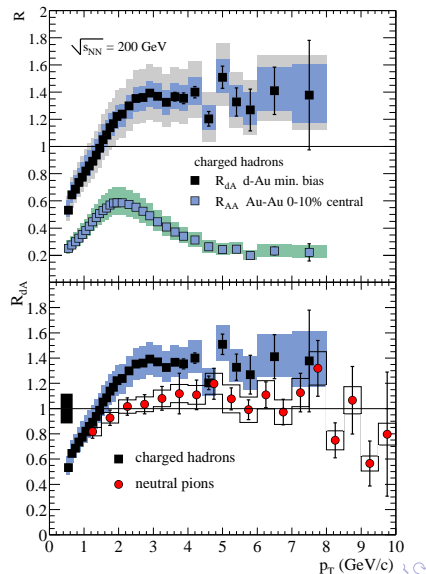
3.8 Nuclear modification factor

The nuclear modification factors R_{AuAu} for central and peripheral collisions (the upper and central two panels), and their ratio (the lower two panels). The measurement of the BRAHMS Collaboration at BNL.

3.8 Nuclear modification factor

The nuclear modification factors R_{dAu} and R_{AuAu} measured by the PHENIX Collaboration at BNL.

4. SPACE-TIME PICTURE OF ULTRA-RELATIVISTIC HEAVY-ION COLLISIONS

The spacetime diagram of ultra-relativistic nuclear collisions. In the center-of-mass frame, partons moving fast hadronize later than those moving slowly. Consequently, at very high energies the evolution of the system at midrapidity is governed by the **longitudinal proper time** $\tau = \sqrt{t^2 - z^2}$, rather than by the ordinary time t. Note, that this picture breaks in the fragmentation regions (i.e., at large values of $|\eta|$) where physical processes have different character.
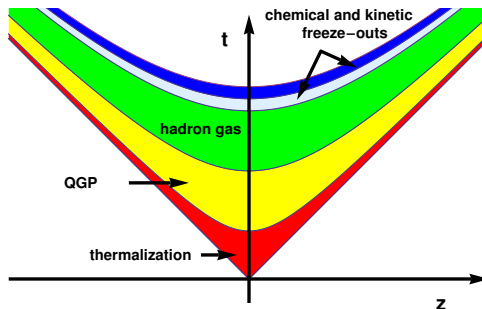
4.1 Particle production processes

The result of the multiple nucleon-nucleon collisions discussed before is that the two colliding nuclei evolve rapidly into an extended, hot and dense system of quarks and gluons.

There exist several frameworks to describe this transition, for example:

1) **QCD string breaking**,

2) **parton cascades models**,

3) **color glass condensate** evolving into **glasma** and later into the **quark-gluon plasma**.

In all cases, the process of the particle production may be characterized by the **decoherence time** τ_{dec} which is required to form the incoherent distribution of quarks and gluons from the highly coherent nuclear wave functions.

Theoretical interpretations of the data measured at RHIC suggest that this time is very short, $\tau_{\mathrm{dec}} \ll 1$ fm. This is so, because the decoherence time τ_{dec} should be smaller than the **equilibration time** τ_{therm}, and the latter has been found to be a fraction of a fermi at RHIC.

4.1.1 String decays

In the **string picture**, the nuclei pass through each other and the collisions of the nucleons lead to the formation of **color strings**.

The strings formed in nucleon-nucleon collisions may be imagined as **quark - diquark pairs connected by the color field**. Such systems may be naively treated as the excited nucleons.

In the next step, the strings decay/fragment forming quarks and gluons or directly hadrons. The hadrons (sometimes clusters of hadrons) are modeled as smaller pieces of the original string. Fragmentation of strings into hadrons is described in the framework of the Monte-Carlo simulations which originate from the **Lund Model**.

space–time picture of hadron formation in the Lund Model
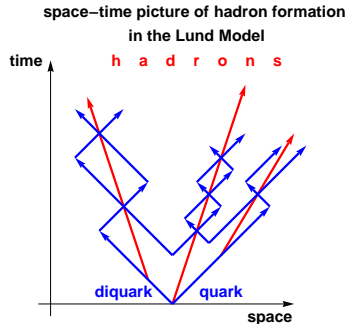
4.1.2 Parton cascade models

The **parton cascade model** is based solely on the perturbative QCD. The colliding nuclei are treated as clouds of quarks and gluons which penetrate through each other. Multiple hard scatterings between partons as well as the gluon radiation produce large energy and entropy density.

The initial state is viewed as an ensemble of quarks and gluons determined by the **quark and gluon distribution functions** $q_f(x, Q^2)$ and $g(x, Q^2)$. The **Bjorken variable** x is defined as the ratio of the longitudinal momentum of the constituent of a hadron to the hadron longitudinal momentum in the reference frame where the hadron has very large energy.

The quantity Q^2 is the **parton virtuality**. The fact that partons are confined in hadrons and cannot exist as free particles implies that they propagate off-shell and Q^2 is an additional independent variable.

4.1.2 Parton cascade models vs. string models

It is important to emphasize that both the string approach and the parton cascade model encounter conceptual problems and limitations. The string picture becomes invalid at very high energies, when the strings overlap and cannot be treated as independent objects. On the other hand, the parton approach is invalid at lower energies, where parton scatterings involve momentum transfers which are too small to be described by perturbation theory.

string models = soft processes

parton cascades = hard processes

4.1.3 Color Glass Condensate

The color electric and magnetic fields describing low x gluons of the **color glass condensate (CGC)** before the collision exist only in the sheets and are mutually orthogonal.
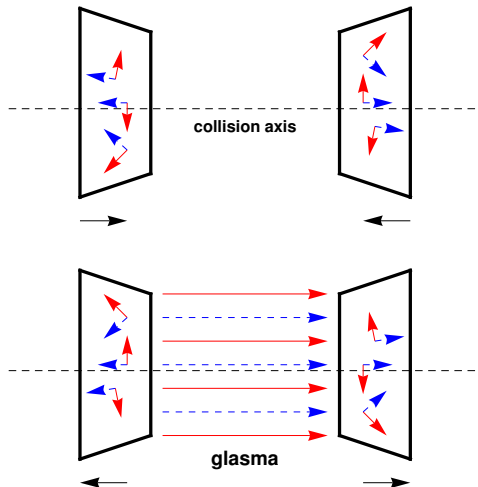
After the collision, in addition to the transverse CGC fields on the sheets there are longitudinal color electric and magnetic fields forming **glasma**.

The glasma fields decay due to the classical rearrangement of the fields into radiation of gluons.

4.2 Thermalization

The experimental data obtained in the RHIC experiments favor a very short thermalization/equilibration time, $\tau_{\mathrm{therm}} < 1$ fm. The **support for this idea comes mainly from applications of relativistic hydrodynamics** which successfully describes the data if one assumes an early starting time of hydro $\tau_{\mathrm{i}} < 1$ fm ($\tau_{\mathrm{therm}} \leq \tau_{\mathrm{i}}$).

Since the final multiplicities are are determined mainly by the number of wounded nucleons, it is reasonable to assume that the initial entropy density of the thermalized system is proportional to the density of wounded nucleons.

$$\sigma_{\mathrm{i}}(\mathbf{x}_\perp) \propto \overline{w}(\mathbf{x}_\perp)$$

4.2 Thermalization: initial conditions for hydrodynamics

The typical arrangement of the coordinate system in the transverse plane. The impact vector, denoted by the dashed arrow, lies in the reaction plane along the x-axis, $\mathbf{b} = (b, 0)$.

The center of the nucleus B has the coordinates $(b/2, 0)$, while the center of the nucleus A is located at $(-b/2, 0)$.

The position of the wounded nucleon is given by the two-dimensional vector $\mathbf{x}_\perp = (x, y)$.
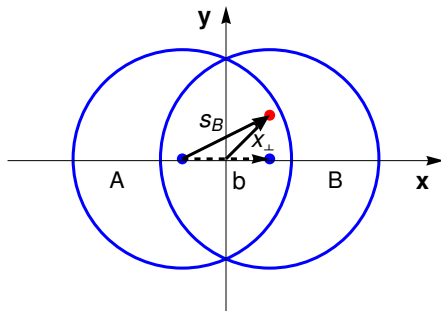
4.2 Thermalization: initial conditions for hydrodynamics

The average density of the wounded nucleons in the nucleus B at the transverse position $\mathbf{x}_\perp$ is

$$\overline{w}_B\left(\mathbf{x}_\perp\right) = B\, T_B\left(-\frac{\mathbf{b}}{2} + \mathbf{x}_\perp\right)\left\{1 - \left[1 - \sigma_{\rm in}\, T_A\left(\frac{\mathbf{b}}{2} + \mathbf{x}_\perp\right)\right]^A\right\}. \tag{45}$$

The average density of the wounded nucleons in the nucleus A is analogous

$$\overline{w}_A\left(\mathbf{x}_\perp\right) = A\, T_A\left(\frac{\mathbf{b}}{2} + \mathbf{x}_\perp\right)\left\{1 - \left[1 - \sigma_{\rm in}\, T_B\left(-\frac{\mathbf{b}}{2} + \mathbf{x}_\perp\right)\right]^B\right\}. \tag{46}$$

For the collision of two nuclei, $A + B$, one may use the final expression in the form

$$\overline{w}\left(\mathbf{x}_\perp\right) \;=\; \overline{w}_A\left(\mathbf{x}_\perp\right) + \overline{w}_B\left(\mathbf{x}_\perp\right). \tag{47}$$

In the case of the binary collisions, similar geometrical considerations lead to the formula

$$\overline{n}\left(\mathbf{x}_\perp\right) = \sigma_{\rm in}\, A\, B\, T_A\left(\frac{\mathbf{b}}{2} + \mathbf{x}_\perp\right) T_B\left(-\frac{\mathbf{b}}{2} + \mathbf{x}_\perp\right). \tag{48}$$

We recall that $\sigma_{\rm in}$ in Eqs. (45), (46), and (48) is the nucleon-nucleon inelastic cross section.

4.2 Thermalization: initial conditions for hydrodynamics

For boost-invariant systems with vanishing baryon chemical potential one usually assumes that either the initial entropy density, $\sigma_i(\mathbf{x}_\perp) = \sigma(\tau_i, \mathbf{x}_\perp)$, or the initial energy density, $\varepsilon_i(\mathbf{x}_\perp) = \varepsilon(\tau_i, \mathbf{x}_\perp)$, are directly related to the density of **sources of particle production**, $\rho_{\rm sr}(\mathbf{x}_\perp)$.

The sources considered in this context are **wounded nucleons** or **binary collisions**. The symmetry with respect to the Lorentz boosts along the collision axis means that it is sufficient to consider all these quantities in the plane $z = 0$. In general, a mixed model is used, with a linear combination of the wounded-nucleon density $\overline{w}(\mathbf{x}_\perp)$ and the density of binary collisions $\overline{n}(\mathbf{x}_\perp)$. This leads to the two popular choices:

$$\sigma_i(\mathbf{x}_\perp) \ \propto \ \rho_{\rm sr}(\mathbf{x}_\perp) = \frac{1-\kappa}{2}\,\overline{w}(\mathbf{x}_\perp) + \kappa\,\overline{n}(\mathbf{x}_\perp) \tag{49}$$
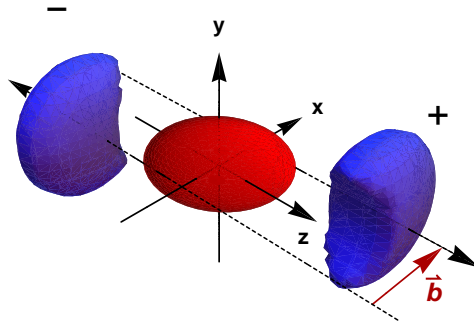
or

$$\varepsilon_i(\mathbf{x}_\perp) \ \propto \ \rho_{\rm sr}(\mathbf{x}_\perp) = \frac{1-\kappa}{2}\,\overline{w}(\mathbf{x}_\perp) + \kappa\,\overline{n}(\mathbf{x}_\perp)\,. \tag{50}$$

4.2 Thermalization: tilted source

Białas and Czyż: analysis of the
deuteron-gold collisions, wounded
nucleons produce particles mainly in the
direction of their motion

P. Bożek: this leads to a tilted source
and explains negative v_1

but all of this requires a hydrodynamic model of expansion...

4.3 Hydrodynamic expansion

The *perfect fluid* is defined formally by the form of its energy-momentum tensor, namely

$$T^{\mu\nu} = (\varepsilon + P)u^\mu u^\nu - Pg^{\mu\nu}, \tag{51}$$

where $g^{\mu\nu}$ is the metric tensor with $g^{00} = 1$, ε is the energy density, P is the pressure, and u^μ is the four-velocity of the fluid element.
Such a form of the energy-momentum tensor follows from the assumption of local thermal equilibrium. Equations of motion of the perfect fluid are obtained from the conservation laws

$$\partial_\mu T^{\mu\nu} = 0. \tag{52}$$

Equations of motion should be supplemented by the equation of state! Otherwise, the system of equations cannot be not closed.

4.3 Hydrodynamic expansion

For systems with non-zero baryon density n, $w = (\varepsilon + P)/n$, $s = \sigma/n$.

Substituting (51) in (52) and using thermodynamic identities gives

$$\frac{d}{d\tau}(wu^{\nu}) \equiv u^{\mu}\partial_{\mu}(wu^{\nu}) = \frac{1}{n}\partial^{\nu}P. \tag{53}$$

The projection of (53) on the fluid four-velocity u_{ν} and the use of thermodynamic identities yields

$$\frac{ds}{d\tau} \equiv u^{\mu}\partial_{\mu}s = 0. \tag{54}$$

4.4 Thermal freeze-out

The *thermal* or *kinetic freeze-out* is the stage in the evolution of matter when the hadrons practically stop to interact. In other words, the thermal freeze-out is a transition from a strongly coupled system (very likely evolving from one local equilibrium state to another) to a weakly coupled one (consisting of essentially free streaming particles).

It is triggered by the expansion of matter, which causes a rapid growth of the mean free path, $\lambda_{\rm mfp}$, of particles. The thermal freeze-out happens when the timescale connected with the collisions, $\tau_{\rm coll} \sim \lambda_{\rm mfp}$, becomes larger than the expansion timescale, $\tau_{\rm exp}$. In this case the particles depart from each other so fast that the collision processes become ineffective. We may formulate this condition as the inequality

$$\tau_{\rm coll} \geq \tau_{\rm exp}. \tag{55}$$

4.4 Thermal freeze-out

The magnitude of the collision time is determined by the product of the average cross section and the particle density,

$$\tau_{\rm coll} \sim \frac{1}{\sigma\, n},$$ (56)

whereas the magnitude of the expansion time is characterized by the divergence of the four-velocity field, u^μ, describing the hydrodynamic flow of matter,

$$\tau_{\rm exp} \sim \frac{1}{\partial_\mu u^\mu}.$$ (57)

Very often a simplified criterion is assumed which says that the thermal freeze-out happens at the time when the mean free path of hadrons is of the same order as the size of the system.

4.5 Chemical freeze-out

A schematic physical picture adopted in the thermal models of particle production. At a certain stage of the evolution of the system, a gas of stable hadrons and resonances is formed. The final (measured) multiplicities of hadrons consist of primary particles, present in the hot fireball, and of secondary particles coming from the decays of resonances.
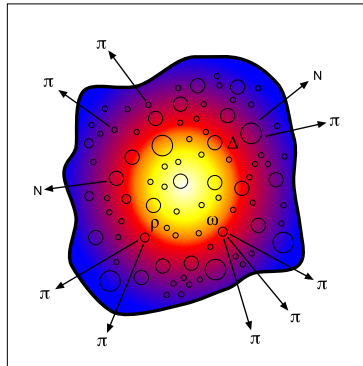
Essentially two parameters, T and μ_B explain the ratios of hadronic abundances! Great success at RHIC!

4.5 Chemical freeze-out

NEWS from the LHC: problems of thermal models with protons!
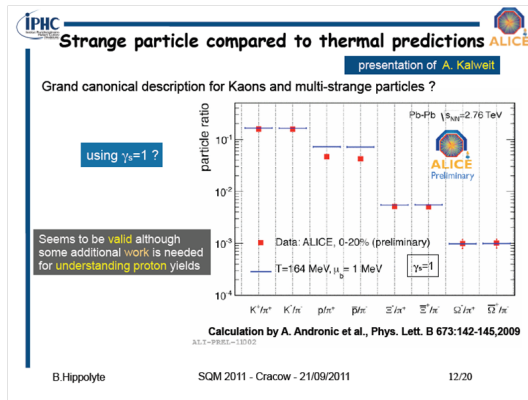
4.6 Hanbury–Brown-Twiss interferometry

The fundamental object in the HBT interferometry is the two-particle correlation function $C(\mathbf{p}_1, \mathbf{p}_2)$, measured for pairs of identical particles such as $\pi^+\pi^+$, $\pi^-\pi^-$, or K^+K^+. In general, it is defined by the expression

$$C(\mathbf{p}_1, \mathbf{p}_2) \quad = \quad \frac{\mathcal{P}_2(\mathbf{p}_1, \mathbf{p}_2)}{\mathcal{P}_1(\mathbf{p}_1)\mathcal{P}_1(\mathbf{p}_2)}, \tag{58}$$

where $\mathcal{P}_1(\mathbf{p})$ is the invariant inclusive one-particle distribution function in the space of rapidity and transverse-momentum,

$$\mathcal{P}_1(\mathbf{p}) \quad = \quad E_p \frac{dN}{d^3p} = \frac{dN}{dy\, d^2p_\perp}, \tag{59}$$

and $\mathcal{P}_2(\mathbf{p}_1, \mathbf{p}_2)$ is the analogous two-particle distribution

$$\mathcal{P}_2(\mathbf{p}_1, \mathbf{p}_2) \quad = \quad E_{p_1} E_{p_2} \frac{dN}{d^3p_1 d^3p_2} = \frac{dN}{dy_1 d^2p_{1\perp} dy_2 d^2p_{2\perp}}. \tag{60}$$

Equations (59) and (60) imply that the correlation function (58) transforms like a Lorentz scalar.
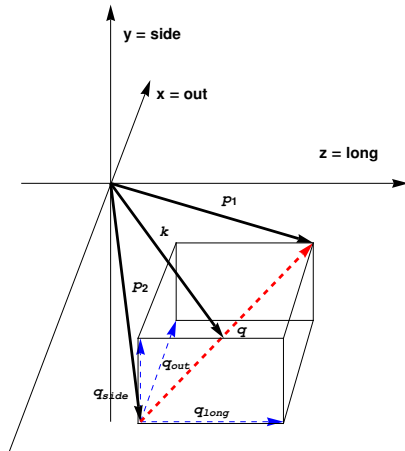
4.6 Hanbury–Brown-Twiss interferometry

In (58) we may use the average momentum

$$\mathbf{k} = \frac{1}{2}\left(\mathbf{p}_1 + \mathbf{p}_2\right), \qquad (61)$$

and the difference of the two momenta

$$\mathbf{q} = \mathbf{p}_1 - \mathbf{p}_2. \qquad (62)$$

The out-side-long coordinate system used in the standard HBT analysis of the correlation functions. The vector $\mathbf{k}$ lies in the $x - z$ plane. By making the Lorentz boost along the collision axis we may also set $\mathbf{k}_\parallel = 0$. In this way we change to the special frame that is called the longitudinally comoving system (LCMS).

4.6 Hanbury–Brown-Twiss interferometry

$$C(k_\perp, \mathbf{q}) = 1 + \lambda \exp\left[-R_{\text{long}}^2(k_\perp)q_{\text{long}}^2 - R_{\text{out}}^2(k_\perp)q_{\text{out}}^2 - R_{\text{side}}^2(k_\perp)q_{\text{side}}^2\right]. \qquad (63)$$

Pion HBT radii vs. $m_T = \sqrt{k_T^2 + m_\pi^2}$ measured by the STAR Collaboration at midrapidity in six different centrality windows.
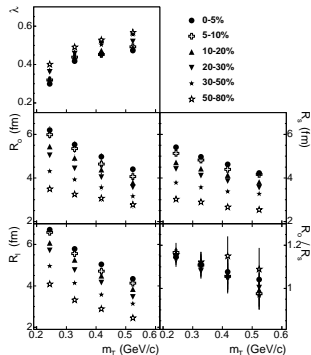
4.6 Hanbury–Brown-Twiss interferometry

NEWS from the LHC: *pp* different from *AA*!